An eight-dimensional quantum mechanical Hamiltonian for X + YCZ_3 system and its applications to H + CH_4 reaction

Rui Liu, Hongwei Xiong, and Minghui Yang

Citation: The Journal of Chemical Physics **137**, 174113 (2012); doi: 10.1063/1.4764358
View online: http://dx.doi.org/10.1063/1.4764358
View Table of Contents: http://aip.scitation.org/toc/jcp/137/17
Published by the American Institute of Physics

An eight-dimensional quantum mechanical Hamiltonian for X + YCZ_3 system and its applications to H + CH_4 reaction

Rui Liu, Hongwei Xiong, and Minghui Yang[a)]
Wuhan Center for Magnetic Resonance, State Key Laboratory of Magnetic Resonance and Atomic and Molecular Physics, Wuhan Institute of Physics and Mathematics, Chinese Academy of Sciences, Wuhan 430071, People's Republic of China

(Received 7 September 2012; accepted 15 October 2012; published online 7 November 2012)

An eight-dimensional quantum mechanical Hamiltonian has been proposed based on Palma and Clary's model in which the non-reacting CZ_3 group keeps a C_{3v} symmetry in the X + YCZ_3 ↔ XY + CZ_3 reaction J. Palma and D. C. Clary [J. Chem. Phys. **112**, 1859 (2000)]. By transforming the original Cartesian coordinate system (x, s) into a scaled polar coordinate system (q, γ), the vibrational Hamiltonian of CZ_3 group is expressed in a simple form with a clear physical picture. This Hamiltonian is used to investigate the H + CH_4 → H_2 + CH_3 reaction on the Jordan-Gilbert potential energy surface. The total reaction probabilities are calculated for the initial ground state, and umbrella, bending, symmetric, and asymmetric stretching excited states of CH_4 with total angular momentum $J = 0$. The integral cross sections for the reaction are also studied for these initial vibrational states with a centrifugal-sudden approximation. The total integral cross sections for the asymmetric stretching vibrational excited state are in good agreement with the experimental observations. The results also showed the difference of dynamical behavior between reactions from symmetric and asymmetric stretching excited states. The thermal rate constants are calculated for the temperature range $T = 250$–2000 K and compared with the experimental and other theoretical results.
 [http://dx.doi.org/10.1063/1.4764358]

I. INTRODUCTION

X + CH_4 is an important type of elementary chemical reaction and has been extensively studied both experimentally[1–18] and theoretically.[19–50] Recently impressive progresses have been made in the experimental studies of H + CH_4,[12] F + CH_4,[17] O + CH_4,[18] and Cl + CH_4[14] reactions and presented new challenges to theoretical chemists.

Due to the quantum nature of chemical reactions, quantum dynamics methods should be employed to obtain the rigorous information. However, the number of the basis functions in quantum dynamics studies increases exponentially with the increase in the size of system and full-dimensional calculations are extremely difficult for polyatomic reactions. Currently the detailed state-to-state quantum dynamics calculations could only be carried out for a few prototype tetra-atomic reactions such as H + H_2O[51–53] and OH + CO.[54] For the reactions including five atoms, the full-dimensional quantum dynamics studies for the reactions such as H + NH_3[55] and H_2 + C_2H[56] have been reported by Yang and Wang, respectively. The initial state-selected total reaction probabilities[55,56] and total integral cross sections (ICSs)[55] were obtained. For a reaction consisting of six atoms, the full-dimensional multi-configuration time-dependent Hartree (MCTDH) methods have been used to evaluate thermal rate constants and cumulative reaction probabilities for $J = 0$ of reaction H + CH_4[48] and the initial state-selected reaction probabilities for the same reaction have also been obtained from a transition state point of view.[49]

Because of the increasing experimental observations of the initial state-selected X + CH_4 reactions,[12,14,15,18] the accurate quantum dynamics calculations with reasonable computational costs are important for the interpretation of experimental results. As a full-dimensional quantum dynamics calculation is difficult to achieve at present, a number of reduced dimensional models have been proposed. The reaction H + CH_4 → H_2 + CH_3 has been viewed as an ideal model for different theoretical approaches. Takayanagi reported a reduced three-dimensional (3D) study by approximating H + CH_4 to a collinear four-atomic system.[20] Yu and Nyman included the umbrella mode in their four-dimensional (4D) treatment with a rotating bond approximation (RBA).[25] Recently, Wang and Bowman have performed a six-dimensional calculation by approximating the three hydrogen atoms in CH_4 group as pseudo-atoms,[31] and the semi-rigid vibrating rotor target (SVRT) model proposed by Zhang has been applied to this reaction in which the reacting polyatomic molecule CH_4 is treated as a semi-rigid vibrating rotor.[34]

Palma and Clary have also suggested a quantum mechanics model for X + YCZ_3 reaction, in which the non-reacting CZ_3 group is restricted to a C_3v symmetry.[23] The exact implementation of this model requires quantum dynamics calculations treated using an eight-dimensional (8D) Hamiltonian. Palma and Clary have studied H + CH_4 and O + CH_4 reactions using a further simplified version, e.g., a collinear four-dimensional Hamiltonian.[24] In this Hamiltonian, the umbrella motion, symmetric, and asymmetric stretching vibrations of

a)Author to whom correspondence should be addressed. Electronic mail: yangmh@wipm.ac.cn.

CH_4 are considered. In the previous studies of these two reactions using a seven-dimensional Hamiltonian, the bending vibration of CH_4 is included and the CH vibration in CH_3 group is frozen.[32,40,46,50] Zhang and co-workers have deduced an eight-dimensional Hamiltonian and used it in a transition state wave packet study.[41] By comparing the eight-dimensional rate constants with the seven-dimensional rate constants, these authors concluded that additional mode has no significant effect on the reactions in the temperature studied.

Experimentally, recent studies have showed some interesting observations about the reaction from the asymmetric stretching vibrational excited state of CH_4.[5,12] Zare and coworkers found a pronounced enhancement of the reaction rate on the excitation of the asymmetric stretching vibrations of CH_4 in the Cl + CH_4 reaction.[5] For the H + CH_4 reaction, they also found that this excitation enhances the overall reaction cross section by a factor of 3 ± 1.5 at a collision energy of 1.5 eV.[12] Because only one stretching mode of CH_4 was considered in the previous seven-dimensional quantum dynamics studies, the reactions from the symmetric or asymmetric stretching vibrational excited states are not distinguishable. Although previous four-dimensional quantum dynamics studies have considered the excitation of asymmetric stretching mode in the calculations, high-dimensional Hamiltonian is still needed to provide accurate predication and interpretation.

In this work, we proposed a new eight-dimensional quantum mechanical Hamiltonian. Comparing with the previous eight-dimensional Hamiltonian,[41] the new Hamiltonian is in a simple form and easy to implement. This Hamiltonian will be employed to investigate the H + CH_4 reaction on the Jordan-Gilbert (JG) potential energy surface.[19] Although several accurate potential energy surfaces have been recently constructed,[38,44,50,57] the JG potential energy surface is employed here to facilitate the comparison between this work and the previous theoretical studies. Section II will describe the details of the Hamiltonian and the basis functions and Sec. III presents the results of time-dependent wave packet studies of the reaction, together with comparison with the previous results using a seven-dimensional Hamiltonian. The conclusion will be given in Sec. IV.

II. THEORY

A. The coordinate system

The eight-dimensional model originally presented by Palma and Clary has been described in a Jacobi coordinate system by us[32,40] and others.[48,50] As shown in Fig. 1, $\boldsymbol{R}$ is the vector from the center of mass of YCZ_3 to X and $\boldsymbol{r}$ is the vector from the center of mass of CZ_3 to Y. The CZ_3 group could be defined with either polar coordinate system (ρ, χ)[41,50] or Cartesian coordinate system (x, s).[23,24] Here, ρ stands for the bond length of CZ and χ is the angle between a CZ bond and vector $\boldsymbol{S}$ which is the symmetry axis of CZ_3; x stands for the distance between atom Z and the symmetry axis $\boldsymbol{S}$ and s is the distance between atom C and the center of three Z atoms. θ_1 is the bending angle between vectors $\boldsymbol{R}$ and $\boldsymbol{r}$ and φ_1 is the azimuth angle of the rotation of YCZ_3 around the vector $\boldsymbol{r}$; θ_2 is the bending angle between vectors $\boldsymbol{r}$ and $\boldsymbol{S}$; and φ_2 is the azimuth angle of the rotation of CZ_3 around vector $\boldsymbol{S}$.

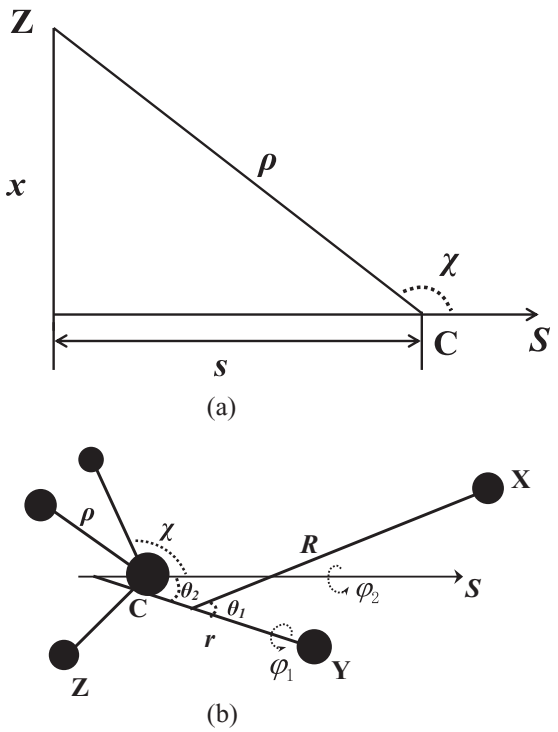

FIG. 1. (a) Cartesian coordinates and polar coordinates of CZ_3 group; (b) Jacobi coordinate system of the X + YCZ_3 model.

Four frames were introduced to describe the angular coordinates and rotation of the system: the space-fixed frame, the body-fixed frame ($XYCZ_3$-fixed frame), YCZ_3-fixed frame, and CZ_3-fixed frame. The z-axis of the body-fixed frame lies along the vector $\boldsymbol{R}$ and the vector $\boldsymbol{r}$ is always in the xz-plane of the frame. The z-axis of the YCZ_3-fixed frame lies along the vector $\boldsymbol{r}$ and the vector $\boldsymbol{S}$ is always in the xz-plane of the frame. The z-axis of the CZ_3-fixed frame lies along its symmetry axis, vector $\boldsymbol{S}$, and the first Z atom is always in the xz-plane of the frame. The four frames form three pairs of related space and body-fixed frames.

B. The model Hamiltonian

By restricting the non-reacting CZ_3 group in C_3v symmetry, the eight-dimensional model Hamiltonian for $XYCZ_3$ system is given by

$$\hat{H} = -\frac{1}{2\mu_R}\frac{\partial^2}{\partial R^2} - \frac{1}{2\mu_r}\frac{\partial^2}{\partial r^2} + \frac{(\hat{J}_{tot} - \hat{J})^2}{2\mu_R R^2} + \frac{\hat{l}^2}{2\mu_r r^2} + \hat{K}^{vib}_{CZ} + \hat{K}^{rot}_{CZ} + V(R, r, x, s, \theta_1, \varphi_1, \theta_2, \varphi_2), \quad (1)$$

where μ_R is the reduced mass of the X + YCZ_3 system and μ_r is the reduced mass of Y + CZ_3. The first two terms are the kinetic energy operators for R and r, respectively; $\hat{J}_{tot}$ is the total angular momentum operator of the system. $\hat{J}$ is the rotational angular momentum operator of YCZ_3 and $\hat{l}$ is the orbital angular momentum operator of atom Y with respect to CZ_3. $\hat{K}^{vib}_{CZ}$ and $\hat{K}^{rot}_{CZ}$ are the vibrational and rotational kinetic energy operators of CZ_3, respectively. Due to the

symmetry required and the definition of the CZ_3-fixed frame, no vibration-rotation coupling exists in this eight-dimensional Hamiltonian. The last term $V(R, r, x, s, \theta_1, \varphi_1, \theta_2, \varphi_2)$ in Hamiltonian is the potential energy.

The vibrational and the rotational kinetic operators could be expressed explicitly with either (ρ, χ) or (x, s) coordinate system. The two operators defined with (x, s) coordinate system are written as[23]

$$\hat{K}_{\mathrm{CZ}}^{rot} = \frac{1}{2I_A}\hat{j}^2 + \left(\frac{1}{2I_C} - \frac{1}{2I_A}\right)\hat{j}_z^2, \tag{2}$$

$$\hat{K}_{\mathrm{CZ}}^{vib} = -\frac{1}{2\mu_x}\frac{\partial^2}{\partial x^2} - \frac{1}{2\mu_s}\frac{\partial^2}{\partial s^2}, \tag{3}$$

where $\hat{j}$ is the rotational angular momentum of CZ_3 and $\hat{j}_z$ is its z-component. The rotational inertia I_A and I_C are defined as[23]

$$I_A = \frac{3}{2}m_z\left[x^2 + \frac{2m_c}{m_c + 3m_z}s^2\right], \tag{4}$$

$$I_C = 3m_z x^2. \tag{5}$$

The reduced mass used here are $\mu_x = 3m_z$ and $\mu_z = 3m_c m_z/(m_c + 3m_z)$. Although these operators defined have simpler forms, the physical picture of (x, s) coordinate system is not clear.

Expressing the vibrational and rotational operators with polar coordinate system (ρ, χ) could provide meaningful interpretation related to the vibrational state of YCZ_3 or CZ_3. In previous seven-dimensional Hamiltonian by further freezing the stretching vibration of CZ bond, the rotational operator $\hat{K}_{\mathrm{CZ}}^{vib}$ keeps its form in Eq. (2) with the rotational inertia I_A and I_C expressed as

$$I_A = \frac{3}{2}m_z\rho^2(\sin^2\chi + 2\cos^2\chi), \tag{6}$$

$$I_C = 3m_z\rho^2\sin^2\chi. \tag{7}$$

While the vibrational operator is[29,31,45,49]

$$\hat{K}_{\mathrm{CZ}}^{vib} = -\frac{1}{2\rho^2}\left(\frac{\cos^2\chi}{\mu_x} + \frac{\sin^2\chi}{\mu_s}\right)\frac{\partial^2}{\partial\chi^2} + \frac{1}{\rho^2}\left(\frac{1}{\mu_x} - \frac{1}{\mu_s}\right)\sin\chi\cos\chi\frac{\partial}{\partial\chi}. \tag{8}$$

While in the eight-dimensional Hamiltonian, the vibrational kinetic operator of CZ_3 group is expressed in a complex form:[41]

$$\hat{K}_{\mathrm{CZ}}^{vib} = -\frac{1}{2}\left(\frac{\sin^2\chi}{\mu_x} + \frac{\cos^2\chi}{\mu_s}\right)\frac{\partial^2}{\partial\rho^2} - \frac{1}{2\rho}\left(\frac{\cos^2\chi}{\mu_x} + \frac{\sin^2\chi}{\mu_s}\right)\frac{\partial}{\partial\rho} - \frac{\sin\chi\cos\chi}{\rho}\left(\frac{1}{\mu_x} - \frac{1}{\mu_s}\right)\frac{\partial^2}{\partial\rho\partial\chi} + \frac{\sin\chi\cos\chi}{\rho^2}\left(\frac{1}{\mu_x} - \frac{1}{\mu_s}\right)\frac{\partial}{\partial\chi} - \frac{1}{2\rho^2}\left(\frac{\cos^2\chi}{\mu_x} + \frac{\sin^2\chi}{\mu_s}\right)\frac{\partial^2}{\partial\chi^2} \tag{9}$$

with the integral element as $\rho\mathrm{d}\rho\mathrm{d}\chi$. This eight-dimensional Hamiltonian with the kinetic operator has been employed in a transition state wave packet study of the $H + CH_4$ reaction.[41]

In this work, a new vibrational kinetic operator for CZ_3 group is presented by transforming Cartesian coordinates (x, s) into scaled polar coordinates (q, γ). Starting from expression in Eq. (3), a new coordinate y is defined as

$$y = \sqrt{\frac{\mu_s}{\mu_x}}s = \sqrt{\frac{m_c}{m_c + 3m_z}}s \tag{10}$$

and the vibrational kinetic operator is then expressed as

$$K_{\mathrm{CZ}}^{vib} = -\frac{1}{2\mu_x}\left(\frac{\partial^2}{\partial x^2} + \frac{\partial^2}{\partial y^2}\right). \tag{11}$$

This is exactly the kinetic operator for a two-dimensional Harmonic oscillator, which could be defined in the scaled polar coordinates (q, γ),

$$\hat{K}_{\mathrm{CZ}}^{vib} = -\frac{1}{2\mu_x}\left(\frac{\partial^2}{\partial q^2} + \frac{1}{q^2}\frac{\partial^2}{\partial\gamma^2} + \frac{1}{q}\frac{\partial}{\partial q}\right) \tag{12}$$

with the integral element as $q\mathrm{d}q\mathrm{d}\gamma$. Here $q = \sqrt{x^2 + y^2}$ and $\gamma = \arctan(y/x)$. In practical application, the basis function for coordinate q is multiplied by a factor of $1/\sqrt{q}$ and the vibrational kinetic operator is expressed as

$$\hat{K}_{\mathrm{CZ}}^{vib} = -\frac{1}{2\mu_x}\left(\frac{\partial^2}{\partial q^2} + \frac{1}{q^2}\frac{\partial^2}{\partial\gamma^2} + \frac{1}{4q^2}\right) \tag{13}$$

with the integral element as $\mathrm{d}q\mathrm{d}\gamma$.

The vibrational kinetic operator could be further divided into two parts, $\hat{K}_{\mathrm{CZ}}^{vib} = \hat{K}_q^{\mathrm{CZ}} + \hat{K}_\gamma^{\mathrm{CZ}}$, with

$$\hat{K}_q^{\mathrm{CZ}} = -\frac{1}{2\mu_x}\frac{\partial^2}{\partial q^2}, \tag{14}$$

$$\hat{K}_\gamma^{\mathrm{CZ}} = -\frac{1}{2\mu_x q^2}\left(\frac{\partial^2}{\partial\gamma^2} + \frac{1}{4}\right). \tag{15}$$

The coordinate q could be viewed as a parameter in Eq. (15) and this operator could be viewed as the kinetic operator of γ solely. The new CZ_3 vibrational kinetic operator is much simpler than the operator expressed in the polar coordinates (ρ, χ). However, this eight-dimensional Hamiltonian cannot be reduced to the seven-dimensional one because the coordinate q does not correspond to the CZ bond whereas the eight-dimensional Hamiltonian expressed in polar coordinates (ρ, χ) could be reduced to seven-dimensional by fixing ρ to its equilibrium value.[32,40,41,50] The factor $\sqrt{\mu_x/\mu_s}$ in Eq. (10) could be viewed as a quantity to estimate the difference between (q, γ) and (ρ, χ). The values of this factor are 1.119 and 1.226 for CH_3 group and CD_3 group, respectively. The vibrational state of CH_4 and HCD_3 can be readily assigned from their wavefunctions solved with the new kinetic operator.

The new form of the vibrational kinetic operator $\hat{K}_{\mathrm{CZ}}^{vib}$ has following desirable properties: (1) It has a simple form as the operator expressed in Cartesian coordinates (x, s). (2) The scaled-polar coordinates have clear meaning as the polar coordinates (ρ, χ) and could facilitate the assignment of the vibrational states of YCZ_3 or CZ_3. (3) Comparing to the polar coordinates (ρ, χ), two scaled-polar coordinates (q, γ) in the new operator $\hat{K}_{\mathrm{CZ}}^{vib}$ could be separated and thus one-dimensional potential-optimized discrete variable representation (PODVR) could be employed to reduce the computational cost.

C. Wavefunction expansion and initial state wavefunction construction

The rotational basis functions used in this work have been reported in previous works[32,40,46,50] and here only a brief introduction is presented. The parity-adapted rotational basis function is written as

$$\Phi_{Jljk}^{J_{tot}M\bar{K}\varepsilon}(\hat{R},\hat{r},\hat{S}) = \sqrt{\frac{1}{2(1+\delta_{\bar{K}0}\delta_{k0})}}\left[\Phi_{Jljk}^{J_{tot}M\bar{K}}(\hat{R},\hat{r},\hat{S}) + \varepsilon(-1)^{J_{tot}+J+l+j+k}\Phi_{Jlj-k}^{J_{tot}M-\bar{K}}(\hat{R},\hat{r},\hat{S})\right] \tag{16}$$

with $\bar{K} = |K|$ and

$$\Phi_{Jjlk}^{J_{tot}MK}(\hat{R},\hat{r},\hat{S}) = \bar{D}_{MK}^{J_{tot}}(\hat{R})Y_{jlk}^{JK}(\hat{r},\hat{S}), \tag{17}$$

$$\bar{D}_{MK}^{J_{tot}}(\hat{R}) = \sqrt{\frac{2J+1}{8\pi^2}}D_{MK}^{*J_{tot}}(\alpha,\beta,\gamma), \tag{18}$$

$$Y_{jlk}^{JK}(\hat{r},\hat{S}) = \sum_m \bar{D}_{Km}^{J}(\hat{r})\sqrt{\frac{2l+1}{2J+1}}\,\langle jml0 \mid Jm\rangle\,\bar{D}_{mk}^{j}(\hat{S}). \tag{19}$$

The time-dependent wavefunction is expanded in the parity-adapted rotational basis functions as

$$\Psi^{J_{tot}M\varepsilon} = \sum_{n_R,n_r,n_q,n_\gamma}\sum_{KJljk} c_{n_Rn_rn_qn_\gamma Jljk}^{J_{tot}MK\varepsilon}(t)G_{n_R}(R)F_{n_r}(r)Q_{n_q} \times (q)H_{n_\gamma}(\gamma)\Phi_{Jljk}^{J_{tot}MK\varepsilon}(\hat{R},\hat{r},\hat{S}). \tag{20}$$

While $c_{n_Rn_rn_qn_\gamma Jljk}^{J_{tot}MK\varepsilon}(t)$ are time-dependent coefficients. n_R, n_r, n_q, and n_γ are labels for the basis functions of R, r, q, and γ respectively. $G_{n_R}(R)$ are sine basis functions and are defined as

$$G_{n_R}(R) = \sqrt{\frac{2}{R_2-R_1}}\sin\frac{n_R\pi(R-R_1)}{R_2-R_1}. \tag{21}$$

The basis functions $F_{n_r}(r)$, $Q_{n_q}(q)$, and $H_{n_\gamma}(\gamma)$ are obtained by solving one-dimensional reference Hamiltonians defined as follows:

$$h_r(r) = -\frac{1}{2\mu_r}\frac{\partial^2}{\partial r^2} + v_r^{ref}(r), \tag{22}$$

$$h_q(q) = -\frac{1}{2\mu_x}\frac{\partial^2}{\partial q^2} + v_q^{ref}(q), \tag{23}$$

and

$$h_\gamma(\gamma,q_{ref}) = -\left(\frac{\partial^2}{\partial\gamma^2}+\frac{1}{4}\right) + 2\mu_x q_{ref}^2 v_\gamma^{ref}(\gamma). \tag{24}$$

While $v_r^{ref}(r)$, $v_q^{ref}(q)$, and $v_\gamma^{ref}(\gamma,q_{ref})$ are the corresponding reference potentials and q_{ref} is a reference value of q to define $h_\gamma(\gamma,q_{ref})$.

For a specific state (J_{tot}, M, ε), the wavefunction is propagated from an initial state wavefunction which is constructed as the direct product of a localized wave packet $G^0(R)$ and the eigen function of YCZ_3 of the specific state (n_0, J_0, K_0, p_0), where n_0, J_0, K_0, and p_0 represent the initial vibrational state, total angular momentum, projection of total angular momentum on the z-axis of the $XYCZ_3$-fixed frame, and the parity of YCZ_3, respectively. In general, $G^0(R)$ is chosen to be a Gaussian function:

$$G^0(R) = (\pi\delta^2)^{-1/4}\exp\left(-\frac{(R-R_0)^2}{2\delta^2}\right)\exp(-ik_0R), \tag{25}$$

where R_0 and δ are the center and width of the Gaussian function; $k_0 = \sqrt{2\mu_R E_0}$; and E_0 is the central energy of the Gaussian function.

The rovibrational eigenfunction of YCZ_3, $\psi_{n_0J_0K_0p_0}^{J_{tot}M\varepsilon}$, is expanded as

$$\psi_{n_0J_0K_0p_0}^{J_{tot}M\varepsilon} = \sum_{n_rn_un_\gamma ljk} d_{n_rn_un_\gamma ljk}^{n_0J_0K_0p_0}F_{n_r}(r)Q_{n_q}(q)H_{n_\gamma}(\gamma) \times \Phi_{J_0ljk}^{J_{tot}M\bar{K}_0\varepsilon}(\hat{R},\hat{r},\hat{S}), \tag{26}$$

which satisfies the following Hamiltonian:

$$\hat{H}_{YCZ_3} = -\frac{1}{2\mu_r}\frac{\partial^2}{\partial r^2} + \frac{\hat{l}^2}{2\mu_r r^2} + \hat{K}_q^{CZ} + \hat{K}_v^{CZ} + \hat{K}_{\mathrm{CZ}}^{rot} + V_{YCZ_3}(r,q,\gamma,\theta_2,\varphi_2) \tag{27}$$

with the potential

$$V_{YCZ_3}(r,q,\gamma,\theta_2,\varphi_2) = V(R=\infty,r,q,\gamma,\theta_1,\theta_2,\varphi_1,\varphi_2). \tag{28}$$

D. Wave packet propagation and reaction flux calculation

The wave packet is propagated using the split-operator propagator:

$$\Psi(t+\Delta) = e^{-iH_0\Delta/2}e^{-iU\Delta}e^{-iH_0\Delta/2}\Psi(t), \tag{29}$$

where the reference Hamiltonian H_0 is defined as

$$H_0 = -\frac{1}{2\mu_R}\frac{\partial^2}{\partial R^2} + h_r^{ref}(r) + h_u^{ref}(\chi) + h_q^{ref}(q) + \frac{1}{2\mu_x q^2}h_\gamma^{ref}(\gamma,q_{ref}) \tag{30}$$

and the reference potential U is defined as

$$U = \frac{(\hat{J}_{tot}-\hat{J})^2}{2\mu_R R^2} + \frac{\hat{l}^2}{2\mu_r r^2} + \hat{K}_{\mathrm{CZ}}^{rot} + V(R,r_1,q,\gamma,\theta_1,\varphi_1,\theta_2,\varphi_2) - v_r^{ref}(r) - v_q^{ref}(q) - \frac{q_{ref}^2}{q^2}v_\gamma^{ref}(\gamma). \tag{31}$$

The calculations of total reaction probabilities are exactly the same as in the previous works.[32,40,41,50] For a specific initial state for a whole energy range, the probabilities can be calculated from the time-independent wavefunction at a dividing surface $r = r_s$:

$$P_i(E) = \frac{\hbar}{\mu_r} \mathrm{Im}(\langle \psi_{iE} | \psi'_{iE} \rangle)|_{r=r_s}, \quad (32)$$

where ψ_{iE} and ψ'_{iE} are the time-independent wavefunctions and its first derivative in r. The time-independent wavefunction ψ_{iE} is obtained by a Fourier transformation of the time-dependent wave packet:

$$|\psi_{iE}\rangle = \frac{1}{a_i(E)} \int_0^\infty e^{i(E-H)t/\hbar} |\Psi_i(0)\rangle \, dt \quad (33)$$

and the coefficient $a_i(E)$ is calculated from the overlap between the initial wavefunction $\Psi_i(0)$ and the energy-normalized asymptotic scattering function ϕ_{iE}:

$$a_i(E) = \langle \phi_{iE} | \Psi_i(0) \rangle . \quad (34)$$

III. RESULTS AND DISCUSSIONS

A. Basis set

An L-shaped wavefunction expansion for R and r was used to reduce the size of the basis set.[26] A total of 80 sine basis functions ranging from 3.0 to 15.0 bohr were used for the R basis set expansion with 24 nodes in the interaction region; and 6 and 25 basis functions of r were used in the asymptotic and interaction regions, respectively. For the vibration of CZ_3 group, 4 and 5 basis functions were used for coordinates q and γ, respectively. The size of the rotational basis functions is controlled by the parameters, $J_{max} = 45$, $l_{max} = 27$, $j_{max} = 18$, and $k_{max} = 18$. After considering parity and C_{3v} symmetry, the size of rotational basis functions was 32 164 and the size of the total basis functions was 6×10^8. The initial vibrational states of CH_4 for $J = 0$ were also solved using the basis set above.

B. Total reaction probabilities

The total reaction probabilities are shown in Fig. 2 for nonrotating CH_4 initially in (a) the ground vibrational state (0,0,0,0) with the zero point energy of 4685.83 cm^{-1}, (b) the excited state of umbrella motion (0,1,0,0) with an excitation energy of 1286.42 cm^{-1} (0.160 eV), (c) the bending excited state (0,0,0,2) with an excitation energy of 2516.46 cm^{-1} (0.312 eV), (d) the symmetrical stretching excited state (1,0,0,0) with an excitation energy of 2821.17 cm^{-1} (0.350 eV), and (e) the asymmetrical stretching vibrational state (0,0,1,0) with an excitation energy of 2948.53 cm^{-1} (0.366 eV). This state is one of the triply degenerate asymmetric stretching excited states in the full-dimensional model and a detailed discussion about this state has been given by Palma and Clary.[24]

Figures 2(a) and 2(b) show the total reaction probabilities as a function of the translational energy and total energy measured with respect to CH_4 in the ground state, respectively.

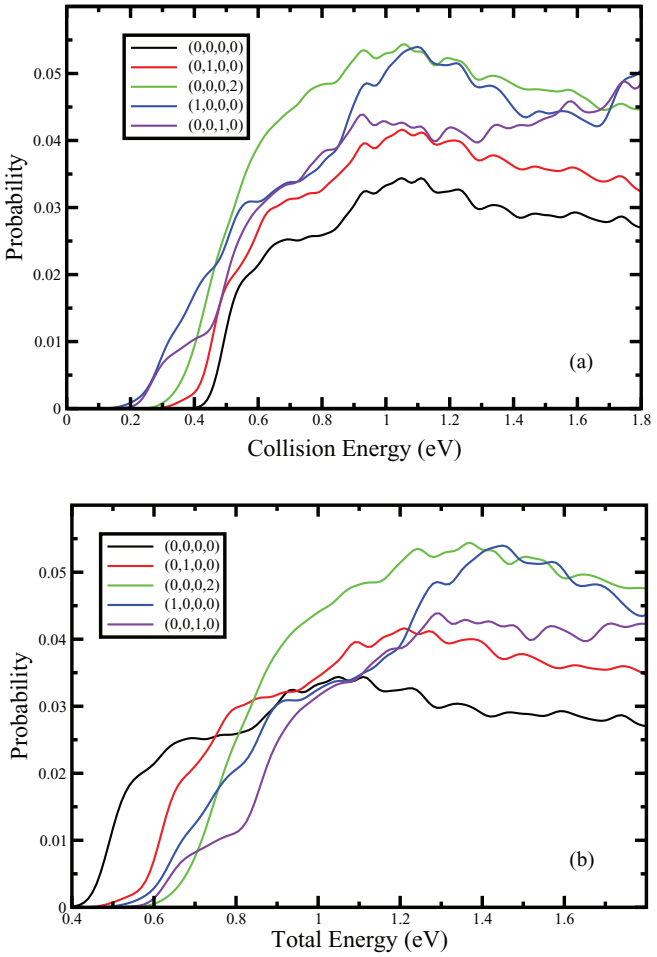

FIG. 2. (a) The total reaction probability for H + CH_4 reaction from the (0,0,0,0), (0,1,0,0), (0,0,0,2), (1,0,0,0), and (0,0,1,0) initial states as a function of translational energy; (b) Same as (a) except plotted as a function of total energy.

From Fig. 2(a), one can see that all vibrational excitations, in particular the symmetric stretching (1,0,0,0) and asymmetric stretching (0,0,1,0) excited states, enhance pronouncedly the reactivity of the system. From Fig. 2(b), the symmetric stretching excitation (1,0,0,0) is the most efficient one in enhancing the reactivity, with 0.202 eV out of 0.350 eV excitation energy deposited to be used to reduce the reaction threshold. The reaction from the asymmetric stretching excited state is very similar to that from the symmetric stretching one, with 0.199 eV out of 0.366 eV used. For the bending excited state (0,0,0,2) about 0.109 eV out of 0.312 eV is used. For the umbrella fundamental excitation (0,1,0,0), however, only 0.045 eV out of 0.160 eV can be used to reduce the reaction threshold. From the Fig. 2(b), one can see that only reaction from the initial ground vibrational state is important at low energies, although all the excitations of CH_4 enhance reactivity.

It is interesting to compare the probability curves obtained in eight-dimensional calculations with that obtained in seven-dimensional (7D) calculations.[31] For the ground state (0,0,0,0) and the umbrella excited state (0,1,0,0), the probability curves calculated with the 8D Hamiltonian are in good agreement with that from the 7D study, indicating that the additional coordinates in the Hamiltonian have minor effect

on the two vibrational modes. For the bending excited state (0,0,0,2), the probability curve is slightly shifted to higher energy, implying that there exists coupling between bending mode and the additional CH stretching mode in the reaction. For two stretching excited states (1,0,0,0) and (0,0,1,0) in the 8D calculations, the probabilities are overall smaller than the stretching state (1,0,0) in the 7D calculation. This may be explained as that the energy could transfer to the CH bond in CH_3 group and thus decrease the reactivity.

It is interesting to note that Palma and Clary had made a similar comparison between the three-dimensional and four-dimensional models.[24] Their study showed that the agreement between the 3D/4D models is very good for the ground state and the probability of 4D model is slightly larger than that of the 3D model. They also showed that the reactivity enhancement from the stretching excitation in the 3D model is larger than that from either the symmetric or asymmetric stretching excitations in the 4D model. As can be seen in Fig. 3(c), the comparison for these stretching excitations between the 7D and 8D models also showed the same behavior. Moreover, they found that the sum of probability curves for two stretching excitations in the 4D model agrees very well with the probability for the stretching excitation in the 3D model (see Fig. 8(c) in Ref. 24). Such an agreement has also been found between the 7D and 8D model in a total energy range from 0.5 to 0.7 eV.

C. Integral cross sections

The ICS for a specific initial state is obtained by summing the total reaction probabilities over all the partial waves:

$$\sigma_i(E) = \frac{1}{2J+1}\frac{\pi}{2\mu E}\sum_{J_{tot}}(2J_{tot}+1)P_i^{J_{tot}}(E). \qquad (35)$$

Since the exact close-coupling calculations for $J_{tot} > 0$ partial waves are expensive, the centrifugal-sudden (CS) approximation is employed in the calculations for $J_{tot} > 0$. The maximum value of J_{tot} needed to converge the integral cross section is $J_{tot} = 50$.

Figure 4(a) shows the integral cross sections for CH_4 initially in five vibrational states as a function of the collision energy. All vibrational excitations enhance the ICS and the behaviors of ICS are very similar to those in the probabilities (see Fig. 2(a)). The ICS as a function of the total energy in Fig. 4(b) showed that the ground state energy dominate the reaction at low total energy and the symmetric stretching excitation (1,0,0,0) and the bending excitation (0,0,0,2) make prominent contributions to the reaction at high energy.

The ICS and the reaction probabilities given in Subsection III D show some oscillations at high energies and the similar oscillations could be observed in the studies with results using the semi-vibrating rotor target model[29] and the seven-dimensional model.[32] While in the recent study with a new interpolated potential energy surface,[36] the probabilities showed a smooth decrease at high energies. For the (0,0,0,0), (0,1,0,0), and (0,0,1,0) states, a platform could be found for ICS curves starting from the total energy of 1.3 eV up to 1.8 eV. Similar behavior has also been observed by Zare and co-workers who found that the enhancement factor of asymmetric stretching vibrational excitation is approximately constant over the 1.52–2.20 eV collision energy range.[12] Particularly at collision energy of 1.52 eV, the ICS for the (0,0,1,0) state is 4.84 a_0^2 while the ICS for the ground state is 2.94 a_0^2. The calculated value of enhancement factor is 1.64,

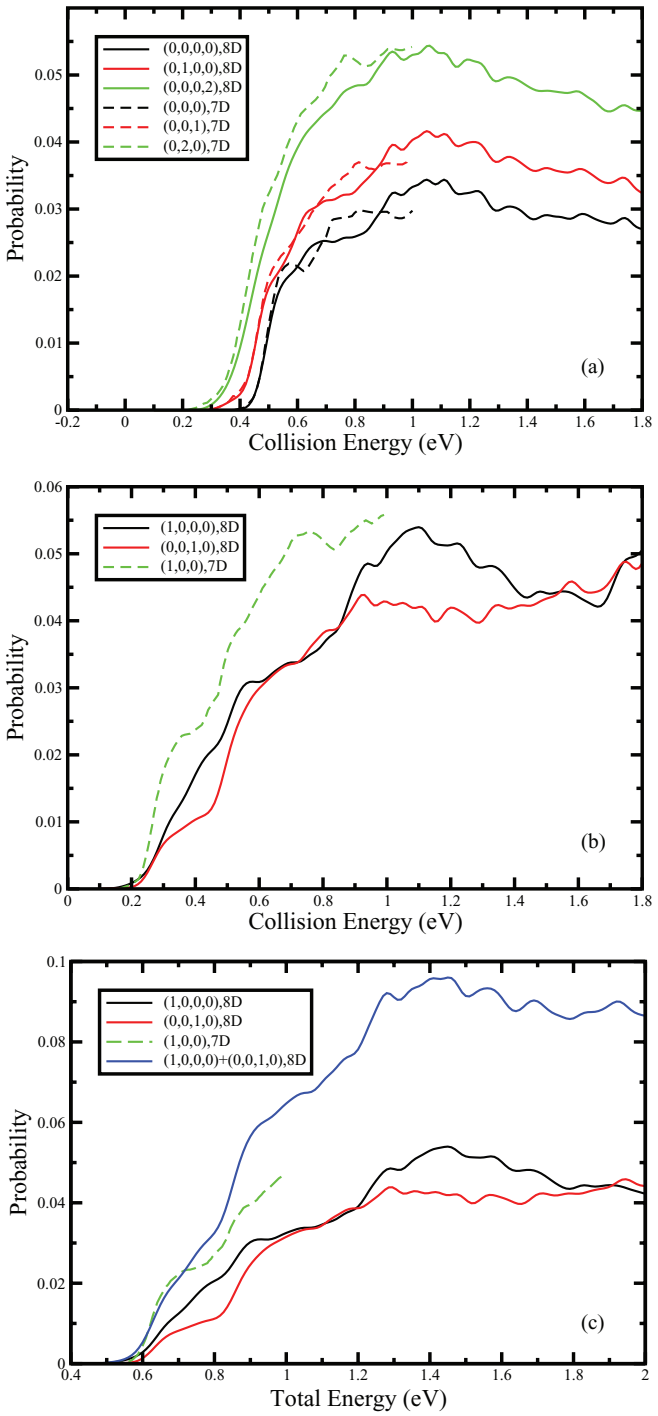

FIG. 3. Comparison of the probabilities based on the seven-dimensional model[31] and the eight-dimensional model. (a) The comparison of total reaction probability for the reactions from (0,0,0,0), (0,1,0,0), and (0,0,0,2) states. (b) The comparison of total reaction probabilities for the reactions from the stretching vibrational excited states in collision energy. (c) The comparison of total reaction probabilities for the reactions from the stretching vibrational excited states in total energy.

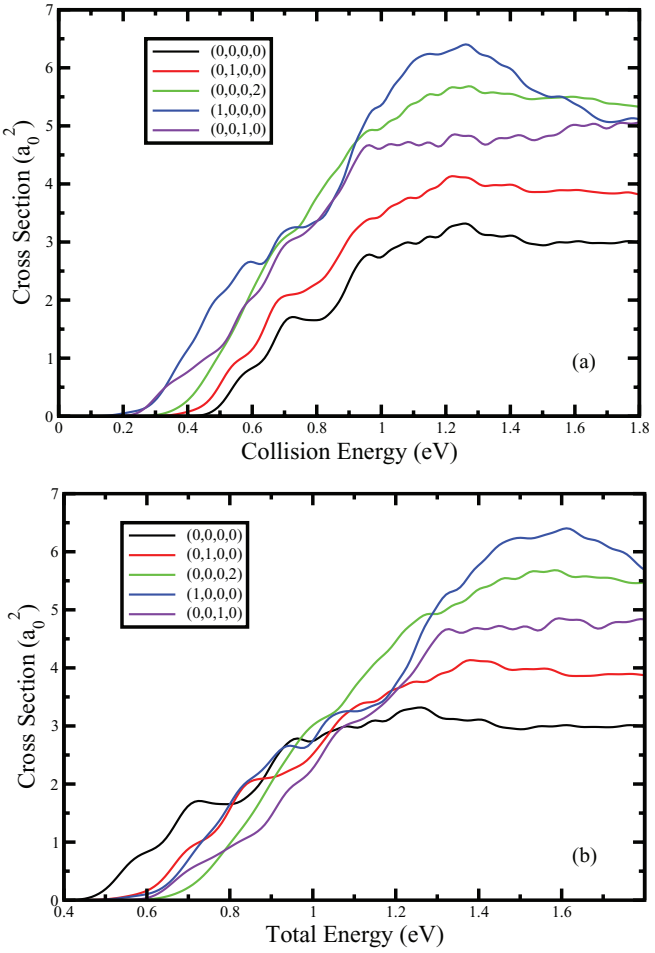

FIG. 4. (a) Integral cross sections for H + CH_4 reaction from the (0,0,0,0), (0,1,0,0), (0,0,0,2), (1,0,0,0), and (0,0,1,0) initial states as a function of translational energy. (b) Same as (a) except plotted as a function of total energy.

which is in agreement with the experimental estimation of 3.0 ± 1.5.

D. Rate constants

The rate constant can be calculated from the cross section:

$$r_i(T) = \left(\frac{8kT}{\pi\mu}\right)^{1/2} (kT)^{-2} \int_0^\infty E_t \exp(-E_t/kT)\sigma_i(E_t)dE_t, \tag{36}$$

or, equivalently, from the total reaction probabilities:

$$r_i(T) = \left(\frac{2\pi}{(\mu kT)^3}\right)^{1/2} \sum_{J_{tot}} (2J_{tot}+1) \times \int_0^\infty \exp(-E_t/kT) P_i^{J_{tot}}(E_t)dE_t. \tag{37}$$

Here, the rate constants are calculated directly from the total reaction probabilities for the ground vibrational state and four excited states and J-shifting approximation was employed here.

The contribution to the thermal rate constants comes mostly from the ground vibrational state in the whole range of calculation temperatures. However, the contribution from the ground state decreases smoothly with the increasing temperature. The contribution from (0,0,0,0) state is approximately 95% at temperature of 250 K and decreases to 37% at temperature of 2000 K. Among the four vibrational excited states, the umbrella excitation (0,1,0,0) has the largest contribution in the whole range of calculation temperatures.

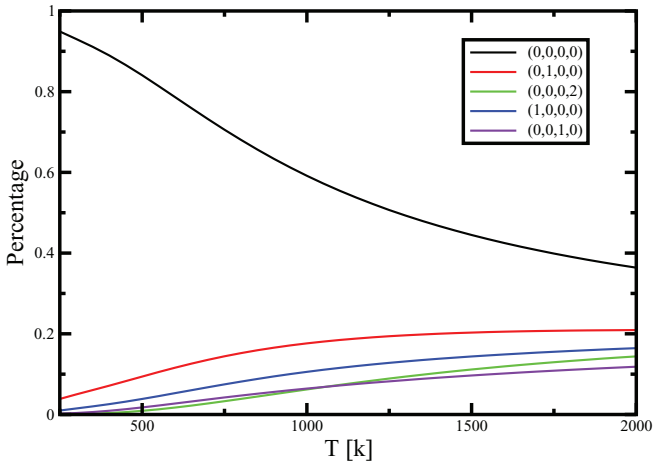

FIG. 5. The percentage of rate constants for reaction from five initial vibrational states.

The rate constants obtained here were compared with the two previous theoretical results and four experimental measurements (Fig. 5). The two theoretical results are obtained from previous seven-dimensional initial state selected wave packet calculation[32] and eight-dimensional transition state wave packet calculation,[41] respectively. Figure 6 showed that the additional coordinates have negligible effect on the rate constants, consistent to the previous eight-dimensional transition state wave packet study.[41] This result could be attributed to the facts that the ground state reaction makes the most prominent contribution and the probabilities are almost the same in seven-dimensional and eight-dimensional calculations.

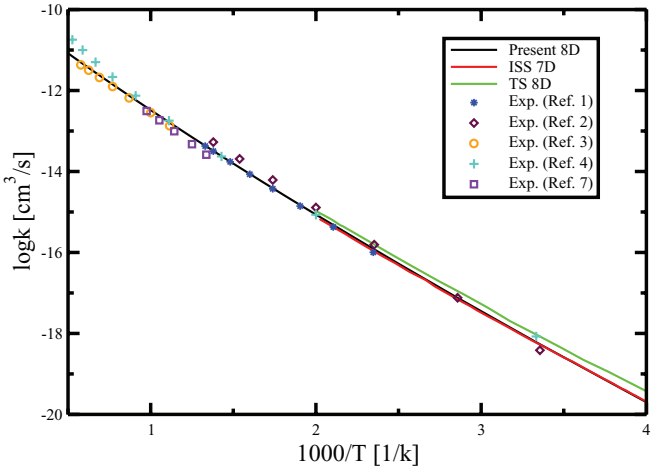

FIG. 6. The thermal rate constants in comparison with the seven-dimensional initial state-selected,[32] eight-dimensional transition state,[41] and experimental rate constants.[1–4,8]

IV. CONCLUSIONS

An eight-dimensional quantum mechanical Hamiltonian for the X + YCZ_3 system has been presented based on a model proposed originally by Palma and Clary.[23] In this model, the non-reactive CZ_3 group keeps a C_{3v} symmetry in reaction and the degree of freedom of the X + YCZ_3 system is reduced to eight dimensions in which two coordinates were used to describe the vibrations of the CZ_3 group. In the previous studies, the two coordinates are expressed as either Cartesian coordinates (x, s) in reduced four-dimensional dynamics studies or polar coordinates (ρ, χ) in reduced seven-/eight-dimensional dynamics studies. This work deduced a set of scaled polar coordinates (q, γ) and presented a new eight-dimensional Hamiltonian. The new Hamiltonian has several desirable properties as: (1) It has a simpler form similar to that expressed in Cartesian coordinates and is easy to implement. (2) It could provide physical interpretation for the vibrational states of YCZ_3 or CZ_3 as the Hamiltonian expressed in polar coordinates (ρ, χ). (3) Two coordinates of the CZ_3 group are separable and one-dimensional PODVR could be employed to reduce the computational costs.

With the eight-dimensional Hamiltonian, the initial state-selected wave packet calculations have been performed for the H + CH_4 reaction on the Jordan-Gilbert PES. The total reaction probabilities and integral cross sections for reactions from the ground and four excited vibrational states of CH_4 are calculated. In particular, the symmetric/asymmetric stretching excitations are included in the high-dimensional initial state-selected dynamics studies. The calculated results showed four interesting features: (1) The ground state reaction makes a predominant contribution although all four excitations enhance the reactions. (2) By comparing the current results with the seven-dimensional calculated results, it showed that the additional coordinates have a almost neglected effect on the rate constants and have a minor effect on the probabilities for reaction from the ground state, the umbrella excited state, and the bending excited state. (3) Two stretching excitations showed different dynamics behaviors and the symmetric stretching excitation is superior in enhancing reactivity than the asymmetric stretching excitation. (4) The vibrational excitation of the asymmetric stretching mode enhances the total integral cross sections by a factor of 1.64 for the collision energy of 1.52 eV. This result is in good agreement with the experimental estimation of 3.0 ± 1.5.[12]

Because all the vibrational modes of YCZ_3 are considered, the new eight-dimensional Hamiltonian could be applied in the study of a number of gas phase reactions, such as Cl + CH_4[14,15] and O + CH_4,[18,40] and other dynamics studies, such as the dissociation of CH_4 on the metal surface.[58–60] The idea in deducing the Hamiltonian with a scaled polar coordinate system could also be extended to developing new methods for H_2 + CH_3 and H + NH_3 reactions.

ACKNOWLEDGMENTS

This work was supported by the National Science Foundation of China (Projects Nos. 20921004, 21073229, and 20833007).

[1] M. J. Kurylo and R. B. Timmons, J. Chem. Phys. **50**, 7056 (1969).
[2] R. R. Baker, R. R. Baldwin, and R. W. Walker, Sym. (Int.) Combust., [Proc.] **13**, 291 (1971).
[3] M. J. Rabinowitz, J. W. Sutherland, P. M. Patterson, and R. B. Klemm, J. Phys. Chem. **95**, 674 (1991).
[4] D. L. Baulch *et al.*, J. Phys. Chem. Ref. Data **21**, 411 (1992).
[5] W. R. Simpson, T. P. Rakitzis, S. A. Kandel, Topaz Lev-On, and R. N. Zare, J. Phys. Chem. **100**, 7938 (1996).
[6] G. M. Sweeney, A. Watson, and K. G. McKendrick, J. Chem. Phys. **106**, 9172 (1997).
[7] W. W. Harper, S. A. Nizkorodov, and D. J. Nesbitt, J. Chem. Phys. **113**, 3670 (2000).
[8] F. Ausfelder and K. G. McKendrick, Prog. React. Kinet. Mech. **25**, 299 (2000).
[9] J. W. Sutherland, M.-C. Su, and J. V. Michael, Int. J. Chem. Kinet. **33**, 669 (2001).
[10] W. Shiu, J. J. Lin, and K. Liu, Phys. Rev. Lett. **92**, 103201 (2004).
[11] W. Shiu, J. J. Lin, K. Liu, M. Wu, and D. H. Parker, J. Chem. Phys. **120**, 117 (2004).
[12] J. P. Camden, H. A. Bechtel, D. J. A. Brown, and R. N. Zare, J. Chem. Phys. **123**, 134301 (2005).
[13] R. Atkinson, D. L. Baulch, R. A. Cox, J. N. Crowley, R. F. Hampson, R. G. Hynes, M. E. Jenkin, M. J. Rossi, and J. Troe, Atmos. Chem. Phys. **6**, 3625 (2006).
[14] H. Kawamata, S. Tauro, and K. Liu, Phys. Chem. Chem. Phys. **10**, 4378 (2008).
[15] H. Kawamata and K. Liu, J. Chem. Phys. **133**, 124304 (2010).
[16] Gábor Czakó, Q. Shuai, K. Liu, and J. M. Bowman, J. Chem. Phys. **133**, 131101 (2010).
[17] F. Wang and K. Liu, J. Phys. Chem. Lett. **2**, 1421 (2011).
[18] J. H. Zhang and K. Liu, Chem. Asian J. **6**, 3132 (2011).
[19] M. J. Jordan and R. G. Gilbert, J. Chem. Phys. **102**, 5669 (1995).
[20] T. Takayanagi, J. Chem. Phys. **104**, 2237 (1996).
[21] H. G. Yu, Chem. Phys. Lett. **332**, 538 (2000).
[22] F. H. Larranaga and U. Manthe, J. Chem. Phys. **113**, 5115 (2000).
[23] J. Palma and D. C. Clary, J. Chem. Phys. **112**, 1859 (2000).
[24] J. Palma and D. C. Clary, Phys. Chem. Chem. Phys. **2**, 4105 (2000).
[25] H. G. Yu and G. Nyman, J. Chem. Phys. **113**, 8936 (2000).
[26] D. H. Zhang, M. A. Collins, and S. Y. Lee, Science **290**, 961 (2000).
[27] F. H. Larranaga and U. Manthe, J. Phys. Chem. **105**, 2522 (2001).
[28] F. H. Larranaga and U. Manthe, J. Chem. Phys. **116**, 2863 (2002).
[29] M. L. Wang and J. Z. H. Zhang, J. Chem. Phys. **116**, 6497 (2002).
[30] J. Palma, J. Echave, and D. C. Clary, J. Phys. Chem. A **106**, 8256 (2002).
[31] D. Y. Wang, J. Chem. Phys. **117**, 9806 (2002).
[32] M. H. Yang, D. H. Zhang, and S. Y. Lee, J. Chem. Phys. **117**, 9539 (2002).
[33] Q. Cui, X. He, M. L. Wang, and J. Z. H. Zhang, J. Chem. Phys. **119**, 9455 (2003).
[34] X. Zhang, G. H. Yang, K. L. Han, M. L. Wang, and J. Z. H. Zhang, J. Chem. Phys. **118**, 9266 (2003).
[35] T. Wu and U. Manthe, J. Chem. Phys. **119**, 14 (2003).
[36] Y. Zhao, T. Yamamoto, and W. H. Miller, J. Chem. Phys. **120**, 3100 (2004).
[37] T. Wu, H. J. Werner, and U. Manthe, Science **306**, 2227 (2004).
[38] X. Zhang, B. J. Braams, and J. M. Bowman, J. Chem. Phys. **124**, 021104 (2006).
[39] T. Wu, H. J. Werner, and U. Manthe, J. Chem. Phys. **124**, 164307 (2006).
[40] M. H. Yang, D. H. Zhang, and S. Y. Lee, J. Chem. Phys. **126**, 064303 (2007).
[41] L. Zhang, Y. Lu, S. Y. Lee, and D. H. Zhang, J. Chem. Phys. **127**, 234313 (2007).
[42] R. van Harrevelt, G. Nyman, and U. Manthe, J. Chem. Phys. **126**, 084303 (2007).
[43] G. Nyman, R. van Harrevelt, and U. Manthe, J. Phys. Chem. A **111**, 10331 (2007).
[44] J. C. Corchado, J. L. Bravo, and J. Espinosa-García, J. Chem. Phys. **130**, 184314 (2009).
[45] S. T. Banks, C. S. Tautermann, S. M. Remmert, and D. C. Clary, J. Chem. Phys. **131**, 044111 (2009).
[46] W. Zhang, Y. Zhou, G. Wu, Y. Lu, H. Pan, B. Fu, Q. Shuai, L. Liu, S. Liu, L. Zhang, B. Jiang, D. Dai, S.-Y. Lee, Z. Xie, B. J. Braams, J. M. Bowman, M. A. Collins, D. H. Zhang, and X. Yang, Proc. Natl. Acad. Sci. U.S.A. **107**, 12782–12785 (2010).
[47] G. Schiffel, U. Manthe, and G. Nyman, J. Phys. Chem. A **114**, 9617 (2010).
[48] G. Schiffel and U. Manthe, J. Chem. Phys. **132**, 084103 (2010).
[49] G. Schiffel and U. Manthe, J. Chem. Phys. **133**, 174124 (2010).

[50]Y. Zhou, B. Fu, C. R. Wang, M. A. Collins, and D. H. Zhang, J. Chem. Phys. **134**, 064323 (2011).
[51]D. H. Zhang and J. C. Light, J. Chem. Phys. **105**, 1291 (1996).
[52]W. Zhu, J. Q. Dai, J. Z. H. Zhang, and D. H. Zhang, J. Chem. Phys. **105**, 4881 (1996).
[53]D. H. Zhang, J. Chem. Phys. **125**, 133102 (2006).
[54]S. Liu, X. Xu, and D. H. Zhang, J. Chem. Phys. **135**, 141108 (2011).
[55]M. H. Yang, J. Chem. Phys. **129**, 064315 (2008).
[56]D. Y. Wang, J. Chem. Phys. **124**, 201105 (2006).
[57]Z. Xie, J. M. Bowman, and X. B. Zhang, J. Chem. Phys. **125**, 133120 (2006).
[58]G. P. Krishnamohan, R. A. Olsen, G.-J. Kroes, F. Gatti, and S. Woittequand, J. Chem. Phys. **133**, 144308 (2010).
[59]B. Jackson and S. Nave, J. Chem. Phys. **135**, 114701 (2011).
[60]M. M. Teixidor and F. Huarte-Larrañaga, Chem. Phys. **399**, 264 (2012).